BRUSH SEAL BRISTLE FLEXURE AND HARD-RUB CHARACTERISTICS

Robert C. Hendricks, Julie A. Carlile, and Anita D. Liang
National Aeronautics and Space Administration
Lewis Research Center
Cleveland, OH 44135

SUMMARY

The bristles of a 38.1-mm (1.5-in.) diameter brush seal were flexed by a tapered, 40-tooth rotor operating at 2600 rpm that provided sharp leading-edge impact of the bristles with hard rubbing of the rotor lands. Three separate tests were run with the same brush accumulating over 1.3×10^9 flexure cycles while deteriorating 0.2 mm (0.008 in.) radially. In each, the test bristle incursion depth varied from 0.130 to 0.025 mm (0.005 to 0.001 in.) or less (start to stop), and in the third test the rotor was set 0.25 mm (0.010 in.) eccentric. Runout varied from 0.025 to 0.076 mm (0.001 to 0.003 in.) radially. The bristles wore but did not pull out, fracture, or fragment. Bristle and rotor wear debris were deposited as very fine, nearly amorphous, highly porous materials at the rotor groove leading edges and within the rotor grooves. The land leading edges showed irregular wear and the beginning of a convergent groove that exhibited sharp, detailed wear at the land trailing edges. Surface grooving, burnishing, "whipping," and hot spots and streaks were found. With a smooth-plug rotor, post-test leakage increased 30 percent over pretest leakage.

INTRODUCTION

High-performance, lightweight engines require compliant seal configurations to accommodate flexible interfaces. Thus, in many aircraft gas turbine engines and other turbomachines brush seal systems are being proposed to replace labyrinth seals because brush seals are compliant and reliable, leak less, cost less, and enhance rotor stability. Brush seals have been the subject of much recent seals research (refs. 1 to 20).

A brush seal system consists of the brush and a hardened rub ring and can be linear, circular, or contoured (see ref. 20 for a review). The bristles are oriented to make an angle of 30° to 50° with the interface, such as the rotor radius for a circular brush. This design allows the bristles to flex when rotor excursions occur without significant damage to either the rotor or the seal.

A typical brush seal configuration, figure 1 (courtesy of Cross Mfg. Ltd. (ref. 1)) consists of (1) a backing plate (like a sealing dam), (2) a circumferential or linear set of packed wires (fibers or bristles), (3) a pinch plate that serves as a retainer for the brush bristles, and (4) an outside diameter surface that fits tightly to the housing (insert in fig. 1). The flexibility of the fibers and implicitly the performance of this seal are governed by many factors as expressed in terms of similitude parameters (refs. 9 and 20). Among these factors are fiber length and diameter, inclination to the moving surface, surface speed, interface friction, seal diameter, fluid properties, packing density, modulus of elasticity, backing plate clearance, and preload or interference fit.

Typically for a circular brush, the wire or brush materials are superalloys and range from 0.05 to 0.07 mm (0.002 to 0.0028 in.) in diameter. The bristles are approximately 0.96 mm (0.38 in.) long and are aligned at 30° to 50° to the shaft in the direction of rotation. Nominally, there are 98 bristles/mm (2500 bristles/in.) of circumference. The interface is characterized by a smooth (4 to 20 rms), hardened rub surface on the shaft (e.g., Al_2O_3 or for short duration the uncoated shaft itself). Because brush seals are contact seals with radial interferences ranging from zero to more than 0.25 mm (0.01 in.), ceramic

coatings and superalloy materials are often used to enhance life and minimize wear at elevated surface speeds, temperatures, and pressure drops.

Although brush seals show great promise for future applications, it must be acknowledged that brush seals are most effective as contact seals and that life and wear rates are major concerns. Whereas bristle blowout will cause excessive leakage, bristle loss and debris have a potential for destructive impact on the powerplant. Thus, the issues of bristle pullout, surface rubbing, bristle wear, and debris are qualitatively addressed in this paper.

The authors are aware that other data exist for ranges of interference fits and other configurations, but the results are proprietary.

APPARATUS

The "drill press" apparatus was similar to that described in reference 2. In the tests of reference 2 the 38.1-mm (1.5-in.) diameter brush seal was fixed in a pressure vessel and the rotor was a smooth-surface, tapered plug turning at 400 rpm. Leakage data at various interferences and eccentricities have been reported (ref. 19).

In the tests described herein the 38.1-mm (1.5-in.) diameter brush seal was again mounted in the pressure vessel that simulated the static housing; but for these tests flutes were machined the length of the plug rotor, providing a set of 40 lands and 40 grooves, or a 40-tooth rotor (fig. 2). The lands were 1.638±0.04 mm (0.0645±0.0015 in.) just above the groove at test 3 and 1.582±0.04 mm (0.0623±0.0015 in.) just below the groove at test 1; see rotor sketch on table I. The groove width (fig. 3) averaged 1.397 to 1.422 mm (0.055 to 0.056 in.) with further dimensions provided in tables I and II. Prior to testing the machining tool marks were clear, being axial in the grooves and circumferential on the lands. This rotor provided 40 impacts of the brush bristles per revolution and was rotated at 2600 rpm.

The 38.1-mm (1.5-in.) diameter brush seal (fig. 4) was damaged in a previous series of tests related to reference 2. The damaged section, although quite small and having a "chewed" appearance, increased seal leakage. The seal could no longer be used for leakage tests but was adequate for the tests herein.

The rotor was AISI 304 stainless steel, and the brush bristles were Haynes 25 in the annealed condition. When stainless steel is rubbed during a machining operation, it tends to change from a "gummy" machining material to a surface-work-hardened material. As a result the bristles would be expected to rub-machine the stainless steel, and in turn the stainless steel would be expected to abrasively remove the bristles.

In test 1 the interference was set at 0.025 to 0.050 mm (0.001 to 0.002 in.) with the groove depth at 0.05 to 0.08 mm (0.002 to 0.003 in.). As expected the bristles rub-machined the rotor.

For test 2 the plug rotor was reset to a portion of the surface that was unrubbed. At that point the groove depth was 0.08 to 0.13 mm (0.003 to 0.005 in.). The interference fit between the rotor lands and the brush was 0.05 to 0.08 mm (0.002 to 0.003 in.).

For test 3 the plug rotor was again reset to a portion of the surface that was unrubbed. The groove depth was 0.178 to 0.254 mm (0.007 to 0.010 in.). For this test the rotor was initially set 0.33 mm (0.013 in.) eccentric, but the rotor rubbed the fence (backing washer) slightly. The fence diameter was 39.2 mm (1.544 in.). The rotor was then reset to an estimated static eccentricity less than 0.25 mm

(<0.010 in.). The dynamic eccentricity was estimated to be less than 1 mm (<0.004 in.). No active clearance measurements were made during these tests; these estimates of eccentricities were made from post-test photographs and static measurements. These settings provided a test with significant rotor impacting and incursion at one portion of the seal and no rubbing contact diametrically opposite to that position.

In tests 1 and 2 the smooth rotor and the 40-tooth rotor were assumed to be interchangeable. The repositioning of the stator for test 3 introduced an unaccountable bias that was estimated in order to correlate the measured flow rates. For test 3 the smooth-rotor initial static eccentricity was estimated to be less than 0.15 mm (<0.006 in.), and after test 3 the estimated static eccentricity was less than 0.25 mm (<0.010 in.).

RESULTS

The results are separated into observations of (1) the brush bristle flexure cycles with associated interface damage to the brush seal and the rotor, and (2) the leakage or performance changes.

Bristle Flexure and Interface Damage

Visualization of the rotor-brush interface at creeping surface speeds (under 10 rpm) revealed little groove penetration. In the impact zone the brush stiffness and the low void did not permit a fully deflected or extended set of bristles at the interface. Instead the impact compacted the bristles in the circumferential direction into the brush and spread the bristles in the axial direction at rate of 40 times per revolution.

Time of testing and brush diameters before and after testing for the three tests are presented in table I; additional dimensions are given in table II. The diameters were obtained by inspecting the brush on an optical comparator before and after each test. The chewed area and a few stray wires served as reference positions for measurements.

Optical inspection of the grooves cut by the brush into the stainless steel rotor (test 1) showed that the cut converged from the leading edge to the trailing edge of the land as the wires (bristles) crossed the rotor (fig. 5). Wire grooves were clear cut and debris was evident, as is better shown in the enlargement (fig. 6).

The following groove extents in millimeters (inches) were measured in test 1:

Width at inlet	1.52 (0.06)
Width at center	1.3 (0.051)
Width at outlet	1.27 (0.05)

For test 2 the inlet region at the land leading edge was extensive and not readily characterized, but a general convergence pattern was evident. Similar behavior at the leading edge was noted for test 3.

In order to corroborate the optical results, profilometer results for a typical tooth of the 40-tooth rotor were taken. Wear area and groove depth estimates are provided in table III. Values for the extent of the groove in millimeters (inches) are shown in figures 7 to 9 at a resolution of 0.02 mm/division.

Width within 0.1 mm of inlet	0.9 (0.035)
Width at center	0.4 (0.016)
Width within 0.08 mm of outlet	0.27 (0.011)

It is evident that the optical values for groove extent were much larger than those from the profilometer. The problem is the scale used in defining the groove depth. For example, at a resolution of 0.01 mm/division the width at the center is 1.15 mm (0.045 in.), but at a resolution of 0.02 mm/division the width at the center is 0.4 mm (0.016 in.). At the smaller resolution the extent of the scratched interface generally agrees with the optical values, but at the larger resolution the extent of the scratched interface is not resolved (i.e., detail is lost).

For the surface asperity resolution used herein the optical method better defined the extent (width) of the damaged interface; the profilometer provided the depth. At one-half the depth resolution only the major grooving was defined.

The first profile, labeled "leading edge," was taken within 0.10 mm (0.004 in.) of the leading edge and shows a broad damage region with deep grooving for test 2 (fig. 8(a)) and test 3 (fig. 9(a)) but a minor amount of material damage for test 1 (fig. 7(a)). The material buildup adjacent to the groove of test 3 probably occurred during rotor-fence rub. The second profile, labeled "mid section," was taken midway between the tooth leading and trailing edges. The damage of test 2 (fig. 8(b)) and test 3 (fig. 9(b)) was severe, and a twofold cut has developed in the rotor during test 2. Again moderate damaged was noted for test 1 (fig. 7(b)). The third profile, labeled "trailing edge," was taken within 5 percent of the trailing edge. The grooving seen in the midsection profile carried through with perhaps some sharpness of the features near the trailing edge (figs. 7(c), 8(c), and 9(c) for tests 1, 2, and 3, respectively).

The brush bristle impact at the leading edge left material deposits that were magnetic (i.e., from the rotor) and rust color (probably Fe_3O_4) with a spongelike (or cauliflower) appearance (fig. 10); these deposits are readily seen at higher magnification (80X) in figure 11. Debris was generated by surface machining grooves, "whipping" of the leading edge, burnishing, and sharp trailing edges. The deposited materials were fine, porous, "greasy" to the fingers, and readily removed from the rotor; removal from the bristles was not straightforward. Standard degreasing cleaned but not thoroughly, and ultrasonic cleaning was not attempted. The reasoning was to see if these deposits would inhibit the responsive character of the bristles. The debris can affect both the response and the leakage, but neither effect was observed in these tests. Further work here is warranted.

These deposits also indicate rapid wear-in with a long oxidation period for the "machined out" material. The materials deposited on the groove wall at the land leading edge (fig. 11) and on the groove wall at the land trailing edge (fig. 12) had little or no structure; the defraction spectra were peakless.

It is speculated that the bristles were dragged across the land, with "machined" material adhering to the bristle and then "impacted" off the bristle at the leading edge of the next tooth. Some of the materials were deposited within the groove. Black nodule-like debris tended to adhere to the groove wall at the land trailing edge. This black material and rust-colored materials formed in the groove at the land leading edge.

Stainless steel work hardens so that the cut grooves were probably harder than the parent stainless steel and would wear the annealed Haynes 25 bristles. The smooth grooves, the hot spots, and the hot streaking may indicate that a thin layer of stainless steel flowed plastically as it was machined out (figs. 13 and 14). Because of the incursive impact of the toothed rotor and the heated interface, the

Haynes 25 bristles could lose strength, erode, fracture, or pull out as massive debris. But no pullouts or massive debris was found after any of the three tests. At higher magnification (200X) the tips still appear intact without fracture, but wear is evident and oxidation debris appears to be well adhered to the surface (fig. 15). As further evidence of the bristle wear an examination of the bristle tip surface revealed tip grooving (fig. 16), and the severe impacting on the bristles is shown by erratic wear notches on the bristle surface (fig. 17).

The trailing edge of the land was "cut" clean by the brush in all three tests (fig. 18) in stark contrast to the erratic leading-edge surface, which was whipped by the bristles (fig. 19). Of interest is the contrast between the land surface cuts. Test 1 surface cuts were a simple wear scar; those of tests 2 and 3 were multiple grooves with complex surfaces and burnishing (fig. 20). The most rotor damage appeared from test 2 and the most brush damage from test 3, where the rotor was set eccentric.

These tests, although preliminary and only qualitative, begin to mitigate the fear of brush seal disintegration through bristle flexing as over 1×10^9 cycles were sustained without failure, fracture, or pullout. However, the required flexures are at least an order of magnitude higher with parameters such as surface speed, temperature, pressure, and materials to be considered.

$$\text{Total flexures} = 222 \text{ hr} \times 60 \text{ min/hr} \times 40 \text{ teeth} \times 2600 \text{ rpm} = 1.38\times10^9$$

$$\text{Required eccentric shaft flexures} = 10\,000 \times 60 \times 1 \text{ (flexure/rotation)} \times 20\,000 \text{ rpm} = 12\times10^9$$

$$\text{Required rotor disk flexures} = 50 \times \text{eccentric shaft flexures}$$

However, bristle flexures raise an equally troubling concern over seal life, because brush seals do wear out. Once these seals begin to reach line-to-line contact, their leakage can be equivalent to that of an advanced labyrinth seal. The sealing margin and competitive edge of the worn brush seal begin to fade. New competitive (lower leakage) configurations for labyrinth, damper, honeycomb, feltmetal, and spiral-groove seals are under investigation. It is clear that long-duration testing at elevated surface speeds and working fluid temperatures are required.

Correlation of Leakage Data

Although not the primary objective of this experiment, overall changes in brush leakage were estimated from flow checks before and after testing. In order to determine these leakages the 40-tooth rotor was replaced with a smooth-surface, tapered rotor. Runout errors resulting from rotor interchange were unresolved as were those associated with the static eccentricity of test 3. Measurements characterizing the rotor and brush before and after testing are given in table I. The average depth of the brush-cut groove as well as the estimated clearances are given in tables II and III.

Leakage is characterized in figure 21 in terms of volumetric flow rate as a function of pressure drop across the brush seal before and after each of the three tests. Both pretest and post-test results are provided in the same figure. Because this brush seal was damaged (see APPARATUS section), absolute leakage measurements would require weighing, but the relative leakage should be accurate. The interference fits for the brush seal leakage data for pretests 1 and 2 were nearly the same, resulting in corresponding leakages. While taking data it was found that the brush would stiffen and the pressure drops would increase. Data points illustrating hystersis (typical in brush seals) are shown. After correcting the post-test 2 data for clearance, these test results agreed with those of post-test 1.

Setting the rotor eccentric in test 3 proved a major problem in cross correlating the leakage results. The estimated initial static eccentricity for the smooth rotor was less than 0.15 mm (0.006 in.), and the smooth rotor and the 40-tooth rotor were assumed to be interchangeable at the same spindle loading. However, the rotor rubbed the fence (backing washer) slightly, requiring an initial static eccentricity of 0.36 mm (0.014 in.) and implying a difference in spindle loading. The rotor was reset to an estimated eccentricity of less than 0.025 mm (0.010 in.). Post-test photographs indicated that the dynamic eccentricity was <0.10 mm (<0.004 in.) and clearly illustrated the fence rub (fig. 22).

For test 3 the repositioning of the stator and the differential spindle loading introduced an unaccountable bias that was difficult to estimate in correlating the leakage results. From the data of reference 19 a relation was found for the change in pressure as a function of eccentricity at a fixed volumetric flow rate. Using this relation and corrections for clearance and assuming a pretest static eccentricity of 0.15 mm (0.006 in.) and a post-test static eccentricity of 0.25 mm (0.010 in.) show that the results of test 3 were overcorrected by 20 percent with respect to the results of tests 1 and 2. Future testing requires instrumentation to overcome these positioning errors. Nevertheless, these leakage data indicate that under conditions of severe brush and rotor wear the brush seal leakage increased 30 percent. And, although brush seal performance degraded, the brush seal did not fail.

SUMMARY OF RESULTS

In three separate tests with a 40-tooth tapered stainless steel rotor operating at 2600 rpm and a 38.1-mm (1.5-in.) diameter brush seal with 0.07-mm (0.0028-in.) diameter annealed Haynes 25 bristles set at a nominal 0.076-mm (0.003-in.) radial interference for each test, the following results were obtained:

1. The bristles withstood over 1×10^9 cycles without pullout, fracture, or massive debris generation.

2. Rotor grooving up to 0.076 mm (0.003 in.) in depth radially with erratic "whipped" leading-edge surfaces followed by convergent grooving to a clean-cut trailing edge was commonplace for each of the three tests.

3. Most of the debris generated was a fine black material that appeared amorphous, but the rust-colored materials were iron rich and magnetic, implying Fe_3O_4. The debris was "cauliflower" in form and highly porous with low adhesion, except for that which was fine enough to adhere to the bristles. Those fines were not readily dislodged. Nonuniform fines (or oxidation) adhering to the bristles tended to separate the bristles, increasing porosity, and would enhance leakage paths.

4. Radial bristle losses up to 0.2 mm (0.008 in.) were demonstrated, which if left uncorrected would lead to equivalent or higher leakages than those of labyrinth seals. Bristle loss at elevated surface speeds and temperatures requires further study.

5. Generated debris can impair bristle motion and alter leakage, but within the limitations of this experiment these considerations were not a problem. They remain as issues to be resolved.

6. Under conditions of severe rotor-stator interface damage, the brush seal leakage performance degraded 30 percent, but the seal did not fail.

REFERENCES

1. Ferguson, J.G.: Brushes as High Performance Gas Turbine Seals. ASME Paper 88-GT-182, 1988.
2. Flower, R.: Brush Seal Development Systems. AIAA Paper 90-2143, 1990.
3. Chupp, R.; and Nelson, P.: Evaluation of Brush Seals for Limited Life Gas Turbine Engines. AIAA Paper 90-2140, 1990.
4. Holle, G.; and Krishnan, M.: Gas Turbine Engine Brush Seal Applications. AIAA Paper 90-2142, 1990.
5. Conner, K.J.; and Childs, D.W.: Brush Seal Rotordynamic Damping Characteristics. AIAA Paper 90-2139, 1990.
6. Hendricks, R.C., et al.: A Bulk Flow Model of a Brush Seal System. ASME Paper 91-GT-325, 1991.
7. Hendricks, R.C., et al.: Some Preliminary Results of Brush Seal/Rotor Interference Effects on Leakage at Zero and Low RPM Using a Tapered-Plug Rotor. AIAA Paper 91-3390, 1991. (Also NASA TM-104396, 1991.)
8. Chupp, R.; and Dowler, C.: Flow Coefficient for Brush Seals. Presented at the 28th Joint Propulsion Conference, Nashville, TN, July 6-8, 1992.
9. Hendricks, R.C., et al.: Brush Seals in Vehicle Tribology. Presented at the 13th Leeds-Lyon Symposium on Tribology, Leeds, England, 1990.
10. Gorelov, G.M., et al.: An Experimental Study of the Rate Characteristics of Brush Seals in Comparison With Labyrinth Seals. Aviats. Tekh., no. 4, 1988, pp. 43-46.
11. Braun, M.J.; Hendricks, R.C.; and Canacci, V.A.: Non-Intrusive Qualitative and Quantitative Flow Characterization and Bulk Flow Model for Brush Seals. Proceedings of Japan International Tribology Conference, ASME, New York, 1990, pp. 1611-1616.
12. Braun, M.J.; Hendricks, R.C.; and Canacci, V.A.: Flow Visualization in a Simulated Brush Seal. ASME Paper 90-GT-217, 1990.
13. Braun, M.J.; Hendricks, R.C.; and Canacci, V.A.: Flow Visualization and Quantitative Velocity and Pressure Measurements in Simulated Single and Double Brush Seals. STLE Tribol. Trans., vol. 34, Jan. 1991, pp. 70-80.
14. Braun, M.; Canacci, V.A.; and Hendricks, R.C.: Flow Visualization and Motion Analysis for a Series of Four Sequential Brush Seals. AIAA Paper 90-2482, 1990.
15. Mullen, R.L.; Braun, M.J.; and Hendricks, R.C.: Numerical Modeling of Flows in Simulated Brush Seal Configurations. AIAA Paper 90-2141, 1990.
16. Hendricks, R.C., et al.: Investigation of Flows in Bristle and Fiberglas Brush Seal Configurations. ISROMAC-4: The Fourth International Symposium of Transport Phenomena and Dynamics of Rotating Machinery, Hemisphere Publ., New York, 1992, pp. 315-325.
17. Carlile, J.A.; Hendricks, R.C.; and Yoder, D.A.: Brush Seal Leakage Performance With Gaseous Working Fluids at Static and Low Rotor Speed Conditions. NASA TM-105400, 1992.
18. Braun, M.J.; Hendricks, R.C.; and Yang, Y.: Effects of Brush Seal Morphology on Leakage and Pressure Drops. AIAA Paper 91-2106, 1991.
19. Schlumberger, J.A.; Proctor, M.; and Hendricks, R.C.: Eccentricity Effects on Leakage of a Brush Seal at Low Surface Speeds. NASA TM-105141, 1991.
20. Hendricks, R.C.; Carlile, J.A.; and Liang, A.D.: Some Sealing Concepts - A Review. Part A: Industrial, Proposed and Dynamic; Part B: Brush Seal Systems. ISROMAC-4: The Fourth International Symposium of Transport Phenomena and Dynamics of Rotating Machinery, Hemisphere Publ., New York, 1992, pp. 247-277.

TABLE I.—DIAMETRAL CHANGES AND TEST CYCLE TIMES FOR 38.1-mm (1.5-in.) DIAMETER BRUSH SEAL

[Seal fence inside diameter, 1.543±0.0005 in.]

	Position				Average
	Vertical	Horizontal	Vertical	Horizontal	
	Rotation, deg				
	0		45		
	Brush diameter (from optical comparator inspection), in.				
Before test 1	1.494	1.4918	1.4926	1.4945	1.4932
After test 1[a]	1.497	1.496	1.495	1.495	1.4958
Change, in.	0.003	0.0042	0.0024	0.0005	0.00255
Before test 2	1.495	1.495	1.497	1.496	1.4958
After test 2[b]	1.5058	1.5061	1.5041	1.5037	1.5049
Change, in.	0.0108	0.0111	0.0071	0.0077	0.00918
Before test 3	1.5058	1.5061	1.5041	1.5037	1.5049
After test 3[c]	1.504	1.514	1.512	1.5064	1.5091
Change, in.	−0.0018	0.0079	0.0079	0.0027	0.00418

[a]Total test time, 70.3 hr.

[b]Total test time, 43 hr.

[c]Total test time, 109 hr.

TABLE II.—ADDITIONAL TEST AND GEOMETRY INFORMATION

[Seal fence inside diameter, 1.543±0.0005 in. Dimensions are in inches.]

(a) 40-Tooth rotor

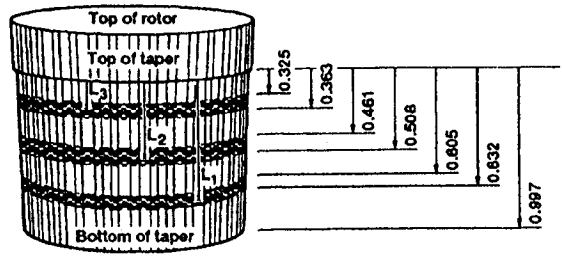

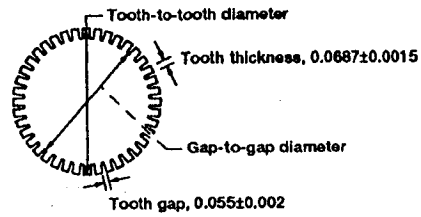

Position	Tooth-to-tooth diameter	Gap-to-gap diamter
Top of rotor	1.523±0.0005	1.485±0.0005
Bottom of rotor	1.491±0.003	1.483±0.003

Test case	Top-of-brush wear surface	Bottom-of-brush wear surface	Average
1	0.605	0.632	0.618
2	.461	.508	.484
3	.325	.303	.344

(b) Smooth rotor

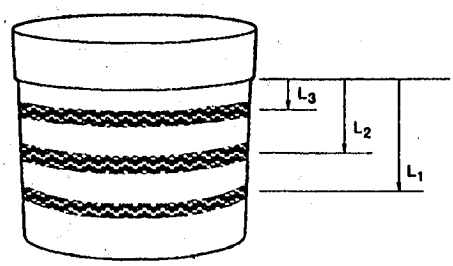

Test case	L[a]	Smooth-rotor diameter	Free brush diameter	Concentric radial clearance	Static eccentricity
Before test 1	L1	1.4992	1.4932	-0.0030	0
After test 1		1.4992	1.4958	-.0017	0
Before test 2	L2	1.5046	1.4958	-0.0044	0
After test 2		1.5046	1.5049	.0001	0
Before test 3	L3	1.5105	1.5049	-0.0028	0.013
After test 3		1.5105	1.5091	-.007	.013

[a]Corresponds to equivalent axial positions of 40-tooth rotor.

TABLE III.—PROFILOMETER RESULTS FOR 40-TOOTH ROTOR,TESTS 1, 2, AND 3

Location	Test	Peak groove depth, μm	Estimated average depth, μm	Wear area, μm^2
Leading edge	1	57	22	24 910
	2	130	95	141 680
	3	130	70	114 370
Midsection	1	30	17	7 652
	2	70	35	37 106
	3	70	27	56 493
Trailing edge	1	25	12	6 610
	2	65	35	48 649
	3	67	30	56 169

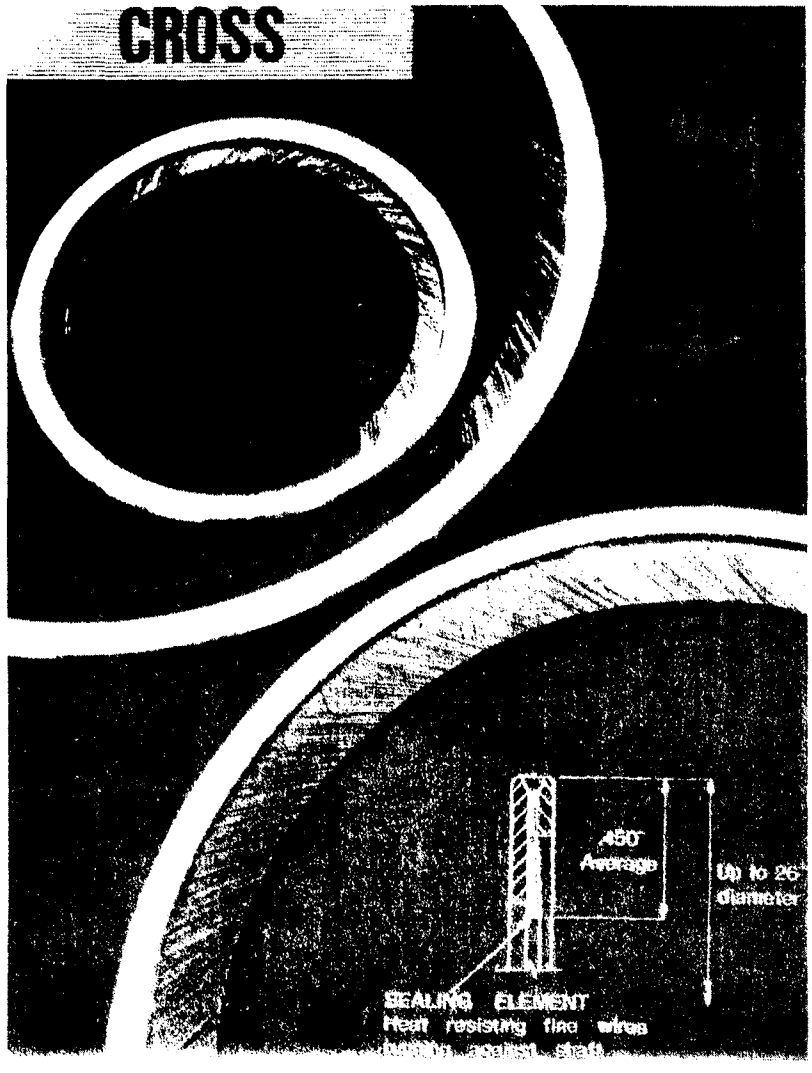

Figure 1.—Circular brush seal. (Courtesy of Cross Mfg. Ltd.)

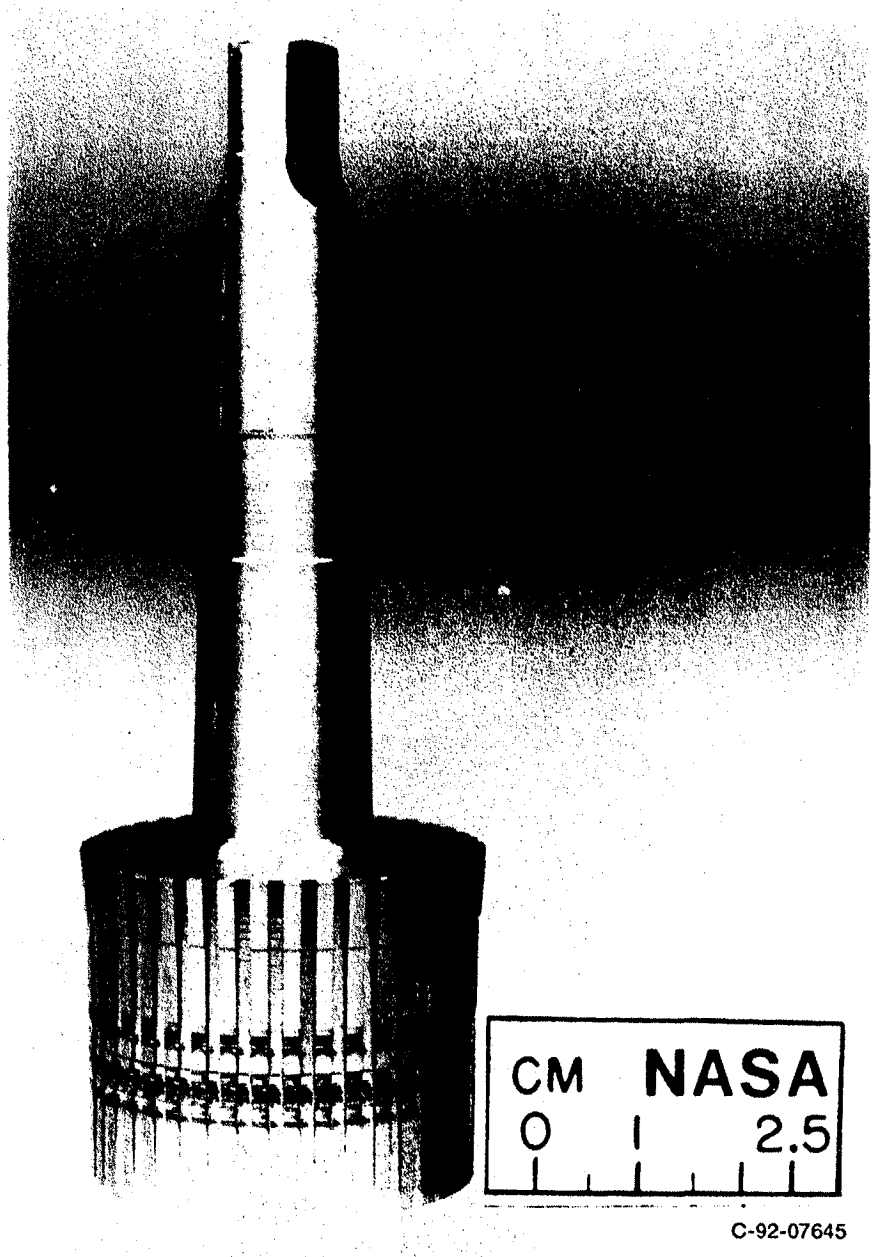

Figure 2.—Geometry of tapered, 40-tooth rotor.

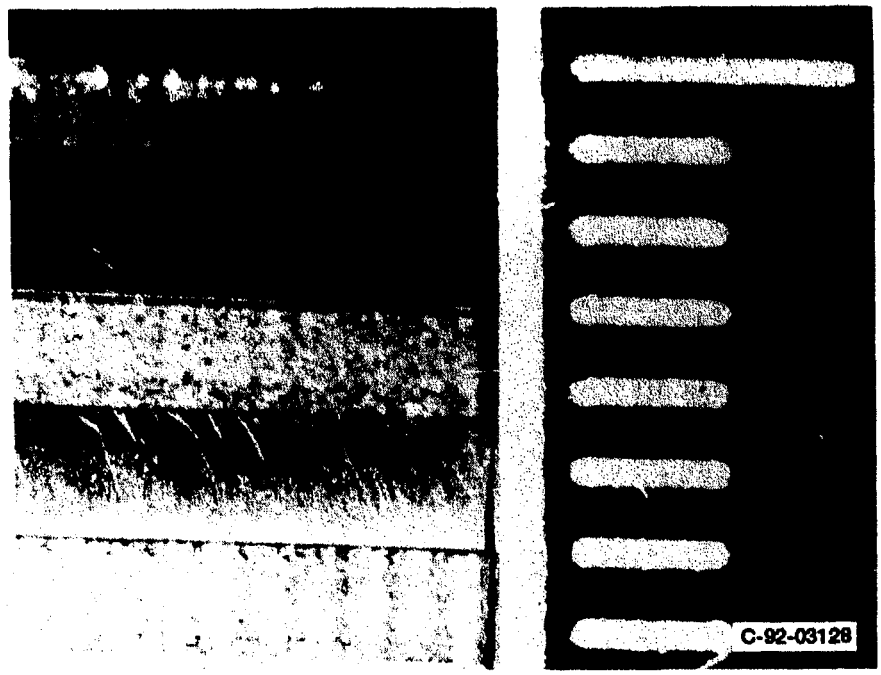

Figure 3.—Rotor prior to tests (40 lands).

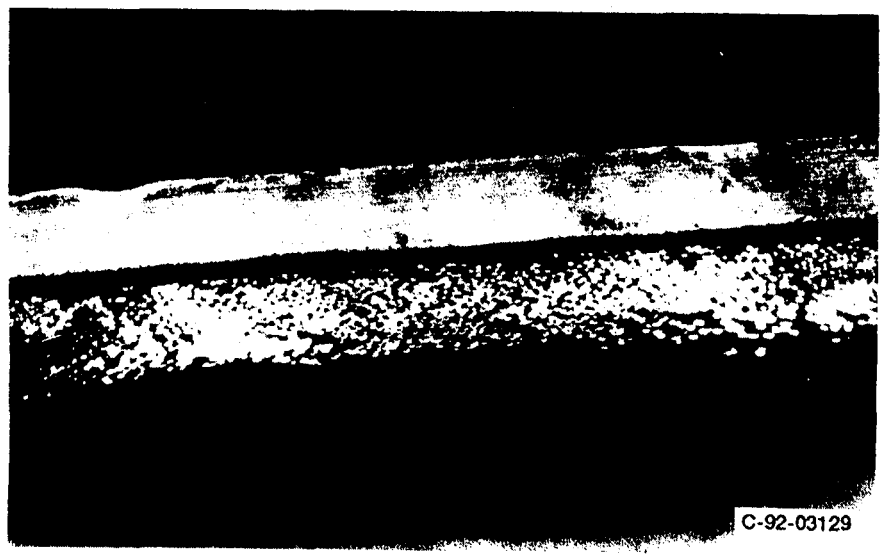

Figure 4.—Brush seal prior to tests (270° mark).

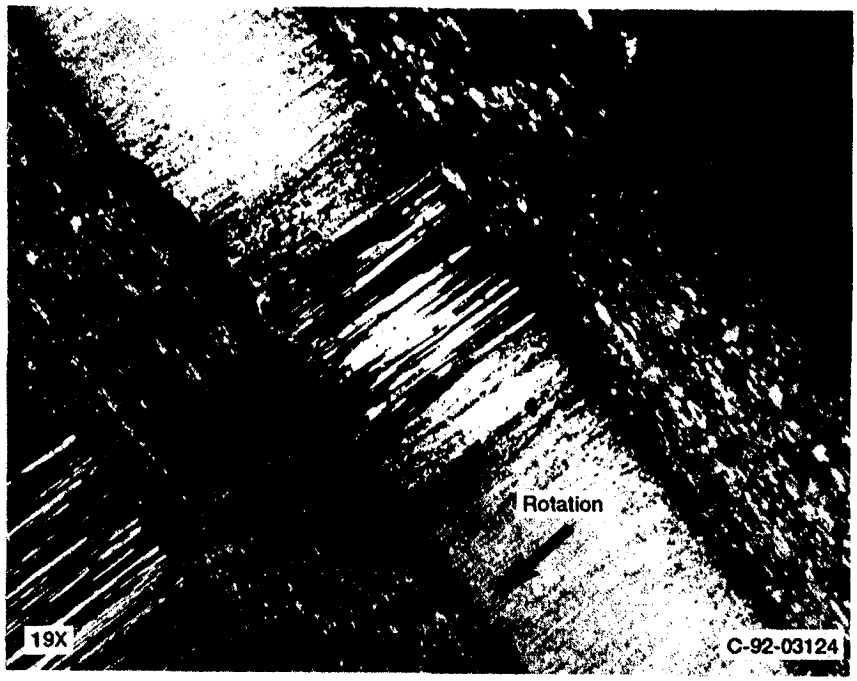

Figure 5.—Rotor surface after test 1. (Arrow shows direction of rotation.)

Figure 6.—Rotor land and groove after test 1.

(c) Trailing edge.

(b) Midsection.

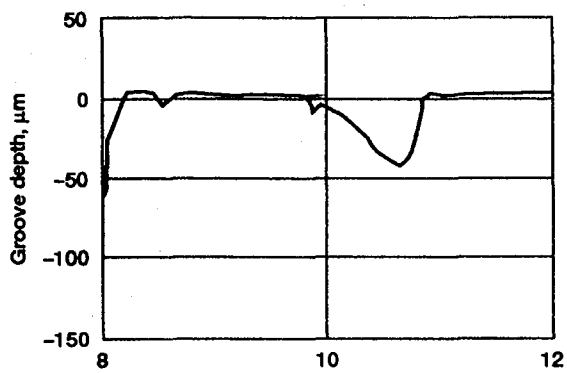

(a) Leading edge.

Figure 7.—Profilometer traces for 40-tooth rotor (test 1).

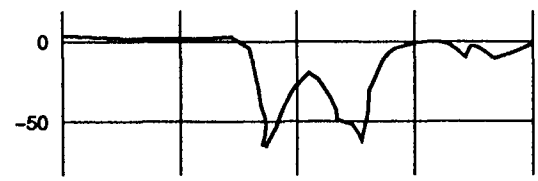

(c) Trailing edge.

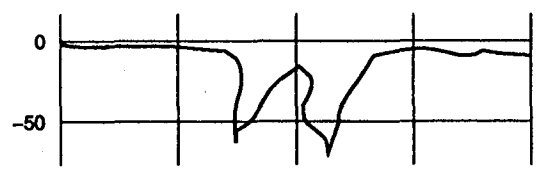

(b) Midsection.

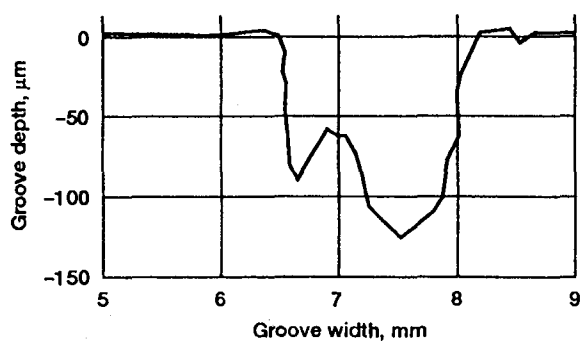

(a) Leading edge.

Figure 8.—Profilometer traces for 40-tooth rotor (test 2).

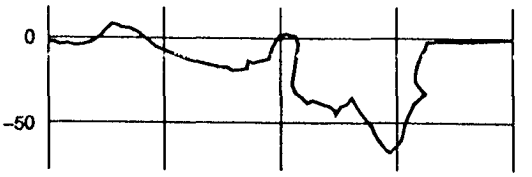

(c) Trailing edge.

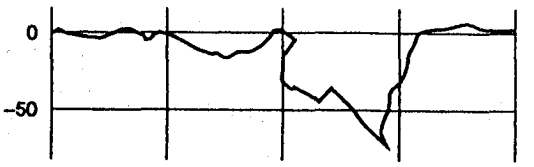

(b) Midsection.

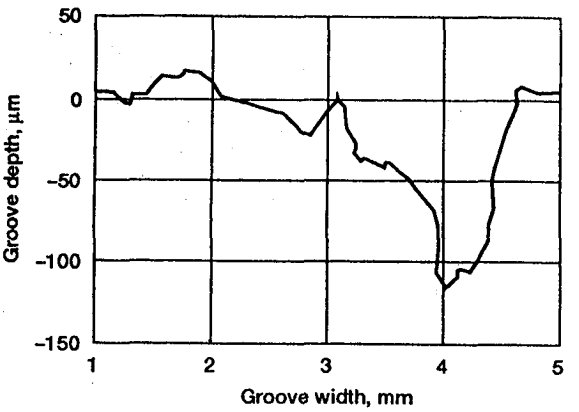

(a) Leading edge.

Figure 9.—Profilometer traces for 40-tooth rotor (test 3).

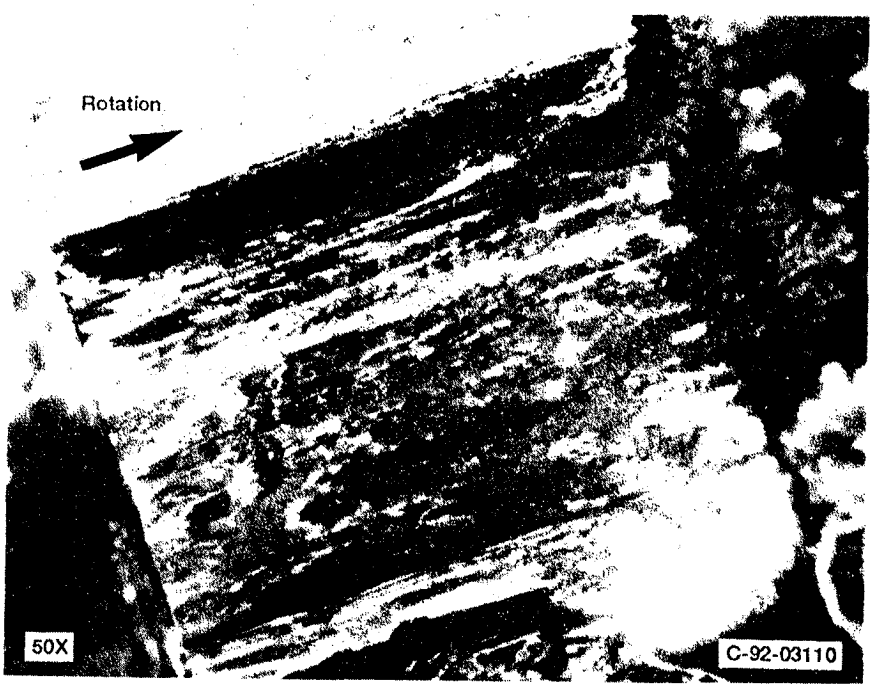

Figure 10.—Rotor land with debris and rub scars (test 2).

Figure 11.—Rotor leading-edge debris formation (test 2).

Figure 12.—Rotor trailing-edge surface grooving and debris (test 3).

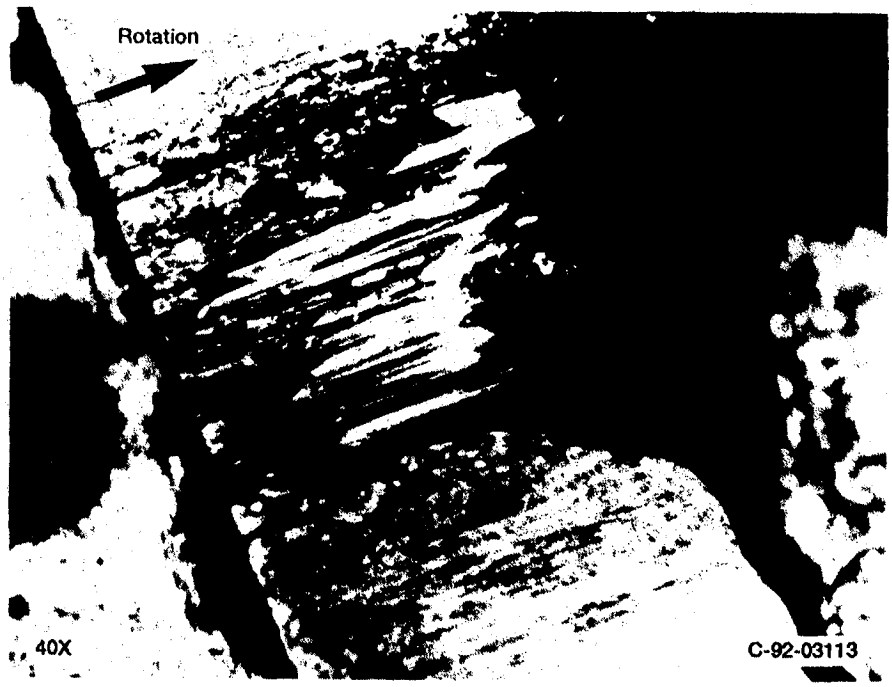

Figure 13.—Rotor leading edge, surface machining, and hot spots (test 3).

Figure 14.—Rotor land hot streaks, hot spots, and surface machining (test 3).

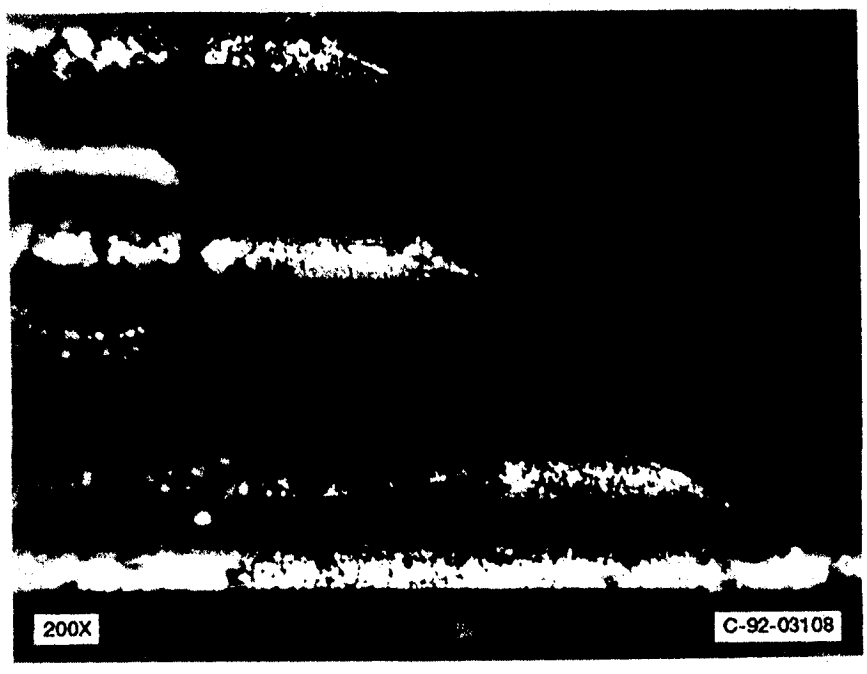

Figure 15.—Brush bristle tips with debris (test 1).

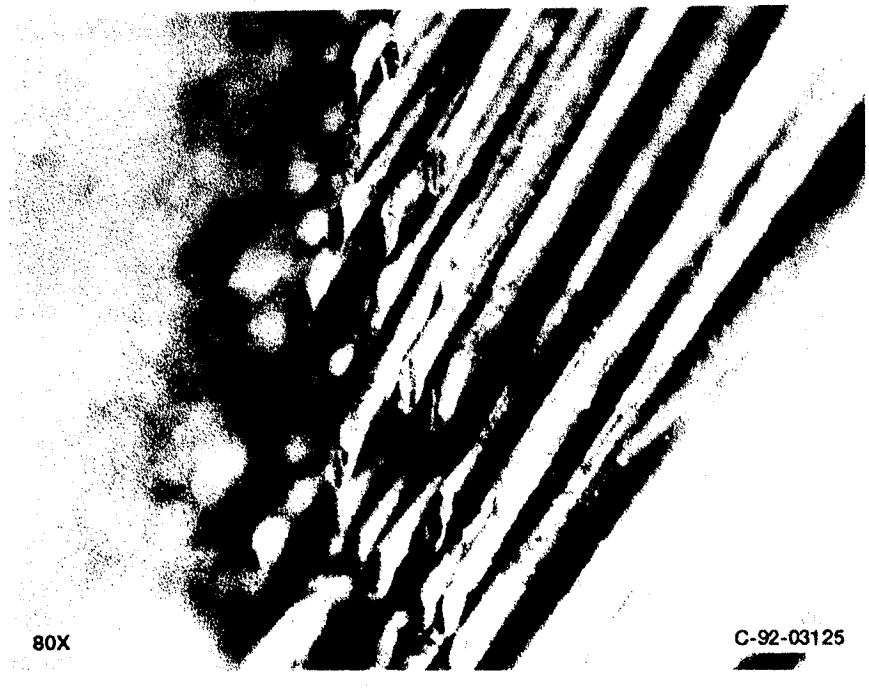

Figure 16.—Brush bristle tip wear patterns (test 2).

Figure 17.—Brush bristle tips and damage (test 1).

Figure 18.—Rotor trailing edge (test 3).

Figure 19.—Rotor leading edge (test 2).

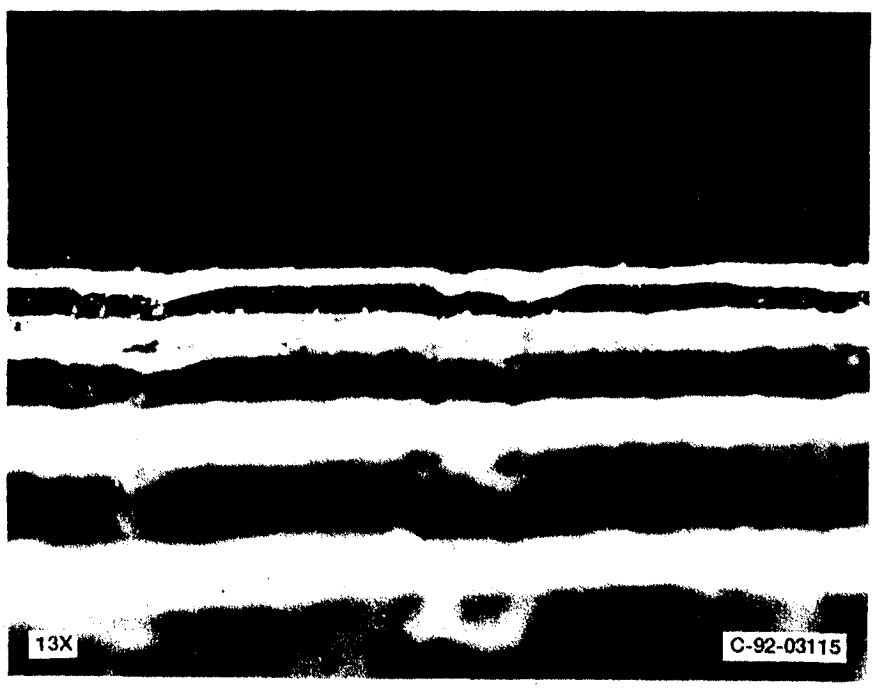

Figure 20.—Rotor trailing edge (tests 1, 2, and 3).

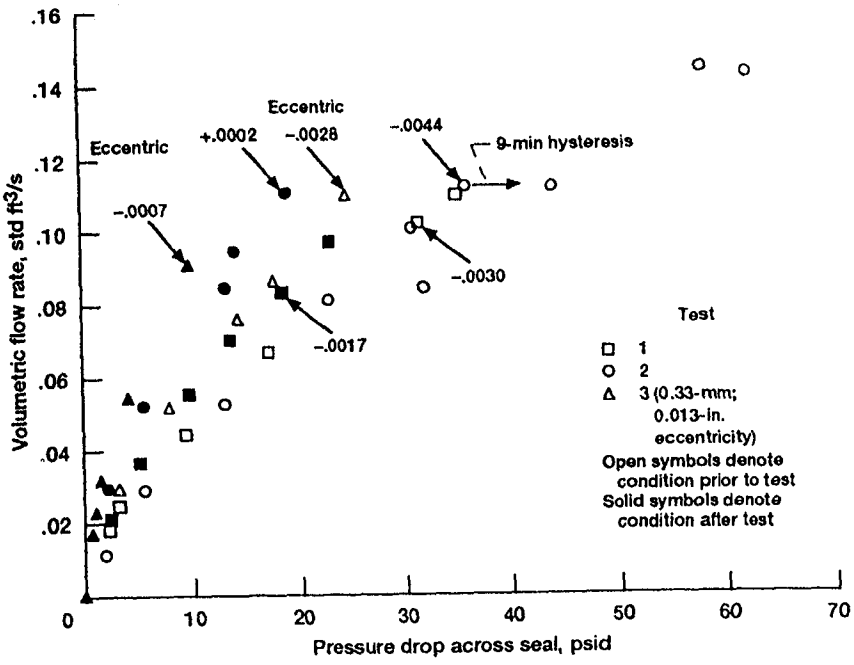

Figure 21.—Pre- and posttest leakage results for smooth rotor.

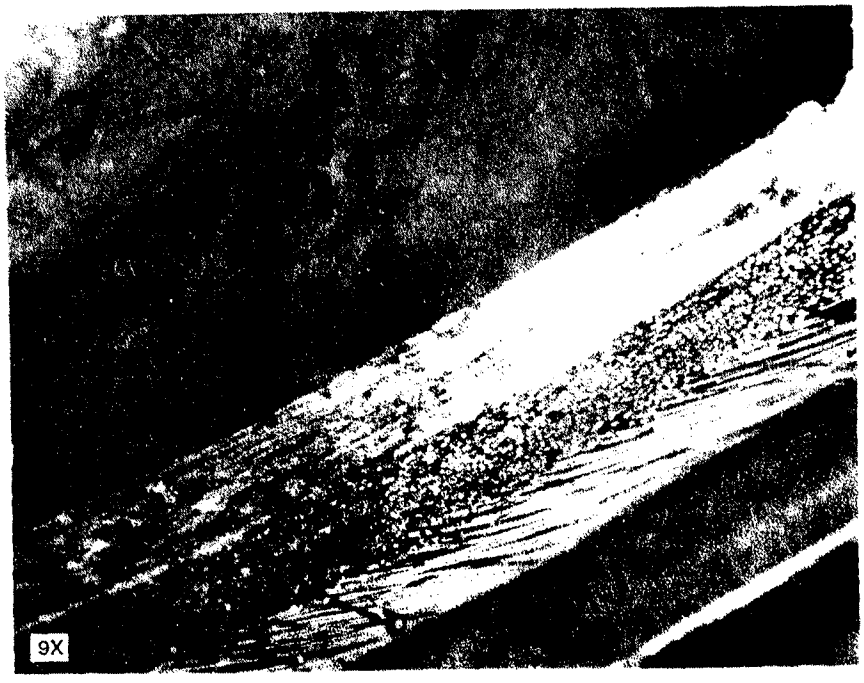

Figure 22.—Fence damage sustained during test 3.